

Baseline Mechanical Characterization of J774 Macrophages

Jonathan Lam,[†] Marc Herant,[‡] Micah Dembo,[‡] and Volkmar Heinrich^{†*}

[†]Department of Biomedical Engineering, University of California, Davis, California 95616; and [‡]Department of Biomedical Engineering, Boston University, Boston, Massachusetts 02215

ABSTRACT Macrophage cell lines like J774 cells are ideal model systems for establishing the biophysical foundations of autonomous deformation and motility of immune cells. To aid comparative studies on these and other types of motile cells, we report measurements of the cortical tension and cytoplasmic viscosity of J774 macrophages using micropipette aspiration. Passive J774 cells cultured in suspension exhibited a cortical resting tension of ~ 0.14 mN/m and a viscosity (at room temperature) of 0.93 kPa·s. Both values are about one order of magnitude higher than the respective values obtained for human neutrophils, lending support to the hypothesis that a tight balance between cortical tension and cytoplasmic viscosity is a physical prerequisite for eukaryotic cell motility. The relatively large stiffness of passive J774 cells contrasts with their capacity for a more than fivefold increase in apparent surface area during active deformation in phagocytosis. Scanning electron micrographs show how microscopic membrane wrinkles are smoothed out and recruited into the apparent surface area during phagocytosis of large targets.

INTRODUCTION

Macrophages are tissue-dwelling immune cells that differentiate from monocytes after extravasation. Their wide-ranging physiological duties encompass both innate and acquired immune functions. For example, macrophages are highly motile cells capable of chemotaxis and pathogen engulfment. They are also key players in the stimulation of specific immune reactions by presenting antigens to lymphocytes.

Due to this multitasking aptitude, macrophage cell lines like J774 or Raw 264.7 are well-established model systems in cell biology and immunology (1–4). Moreover, because macrophage cell lines can easily be maintained and genetically manipulated, they are also increasingly recognized as preferred model systems for quantitative biophysical studies of eukaryotic cell motility and immunomechanics. This common focus of traditionally separate research areas is particularly evident in interdisciplinary efforts to elucidate the mechanistic underpinnings of phagocytosis (5–10).

The biophysical analysis of phagocytosis mechanics (7,8) offers new ways to assess variations in cell motility between different cell types. Understanding the origins of such variations will establish how well insights obtained from experimentally more amenable cell lines carry over to motile cell behavior in humans. Variability in cell motility could stem from differences in the inherent, preprogrammed intracellular response to external stimuli. Alternatively, differences in the baseline mechanical cell properties could modulate an otherwise universal cellular response program.

As a first step toward the distinction between these (not necessarily exclusive) alternatives, we present an in-depth micromechanical characterization of J774 macrophages. It is based on micropipette aspiration (11) of individual cells (Fig. 1) that were cultured in suspension. Two sets of comple-

mentary aspiration experiments were conducted to establish the mechanical behavior of the cell cortex and the cytoplasmic interior of passive macrophages, respectively. Furthermore, we compared the resistance to surface-area expansion of passive cells with the ability of active macrophages to recruit enormous membrane reserves during autonomous deformation.

MATERIALS AND METHODS

J774 macrophage cell line

Mouse macrophages (J774A.1 cell line) were purchased from American Type Culture Collection and cultured in Dulbecco's modified Eagle's medium supplemented with 10% fetal bovine serum (FBS) at 37°C with 5% CO₂ in the atmosphere. The cells were grown in two different ways: adherent to cell-culture flasks, and in suspension. Adherently cultured cells were removed for passage and for experiments by scraping. Alternatively, suspended cells were grown in 50 mL bioreactor tubes with specialized caps that allowed for gas exchange (Techno Plastic Products/Midwest Scientific, St. Louis, MO). The tubes were continually rotated on a rolling apparatus (Stovall, Greensboro, NC) placed in an incubator. The cells were passaged twice per week by centrifugation (at 200 g for 3 min) and resuspension in fresh culture medium.

For each experiment, a small volume (5–10 μ L) of cells was introduced into the experimental chamber, which contained Hanks' balanced salt solution with 10% FBS. Experiments were conducted in Hanks' balanced salt solution either with calcium and magnesium or without, respectively (Sigma-Aldrich, St. Louis, MO). In the latter case, ~ 1 mM EDTA was added to the solution. All experiments were carried out at room temperature.

Preparation of the experiment chamber

Custom microscope chambers designed for automated video-microscope imaging of micropipette-manipulation experiments were machined from polycarbonate (Fig. 1). Lateral chamber dimensions were the same as those of standard microscope slides (25 mm \times 75 mm). The typical chamber thickness was ~ 1.4 mm. A U-shaped cutout sandwiched by top and bottom glass coverslips formed the actual test volume. The front of the chamber remained open for micropipette access. Capillary action retained the buffer solution inside the shallow chamber.

Submitted June 2, 2008, and accepted for publication September 10, 2008.

*Correspondence: vheinrich@ucdavis.edu

Editor: Akihiro Kusumi.

© 2009 by the Biophysical Society
0006-3495/09/01/0248/7 \$2.00

doi: 10.1529/biophysj.108.139154

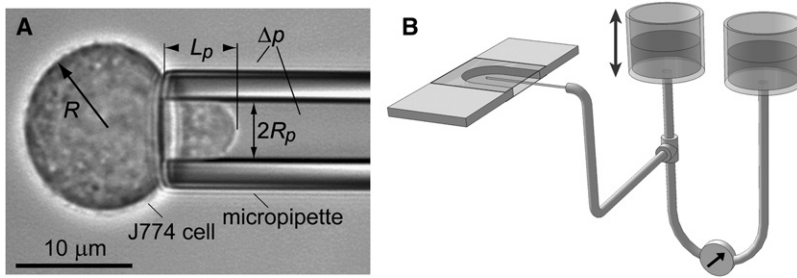


FIGURE 1 Overview of the pipette-aspiration setup. (A) The video micrograph of a pipette-held J774 cell defines the notation used in the text. (B) Glass coverslips form the top and bottom of the U-shaped experiment chamber. The open front allows for pipette access. The pipette is connected via flexible tubing to a pressure-application and measurement system consisting of two vertically movable water reservoirs and a differential pressure transducer.

To prevent cell adherence and activation, the coverslips used as chamber bottoms were passivated by covalent attachment of 2-[methoxy (polyethyleneoxy) propyl] trichlorosilane (PEG-silane, Gelest, Morrisville, PA). Glass coverslips were first washed and plasma cleaned (Harrick Plasma, Ithaca, NY), then placed in a moisture-free argon environment (AtmosBag; Sigma-Aldrich) into a beaker containing PEG-silane dissolved at 2% (vol/vol) in anhydrous toluene (Sigma-Aldrich). The PEG-silane was allowed to bind to the glass surface for 2 h. Subsequently, the coverslips were washed in toluene, dried under a stream of argon, and then dried in an oven at 37°C for 1 h. The PEG-silanized coverslips were stored in a desiccator and used within 2 weeks.

Micropipette aspiration

Our automated micropipette-aspiration setup (Fig. 1) has been described in detail in a previous article (11). To diminish activation of pipette-held J774 cells, the pipettes used in this study were coated with silicon. IMAX-51 glass capillaries (1 mm outer diameter; Kimble, Vineland, NJ) were cut to the desired length (~12 cm) and sonicated in Branson cleaning solution for 5 min. After extensive rinsing with deionized water, the capillaries were pulled to the desired tip diameter and shape on a micropipette puller (model P-87; Sutter Instrument, Novato, CA). They were then postprocessed on a microforge (model MF-900; Narishige, East Meadow, NY) to obtain an evenly broken tip. Typical inner pipette-tip diameters were ~5 μm for cortical-tension measurements, and ~8–11 μm for whole-cell aspiration experiments used to establish the cytoplasmic viscosity of J774 cells.

The cut pipettes were plasma cleaned and then treated with SurfaSil siliconizing fluid (Fisher Scientific, Pittsburgh, PA). The SurfaSil fluid was diluted in toluene to a concentration of 5% (vol/vol). Pipette surfaces were siliconized by repeatedly front-filling each pipette with this solution and then expelling it from the pipette. Finally, each pipette was thoroughly rinsed (first with toluene, then with methanol), and then dried at 100°C for 1 h.

Preparation of phagocytosis target beads

Polystyrene beads (nominal bead diameters 20 and 30 μm; Duke Scientific/Fisher Scientific) were incubated overnight at 4°C with 10 mg/mL bovine serum albumin (BSA) dissolved in phosphate buffered saline (PBS). After three washes with PBS (without BSA), the beads were incubated with mouse monoclonal anti-BSA antibody (Sigma-Aldrich) for 1 h at room temperature. The beads were then washed once more and re-suspended in PBS for storage at 4°C. On days of experiments, small amounts of antibody-coated beads were retrieved, sonicated, and washed in PBS; ~5 μL of bead suspension were introduced into the experimental chamber.

RESULTS AND DISCUSSION

Suppression of cell activation

Consistent, reproducible results in single-cell experiments require that all inspected cells initially be in a comparable “standard” state. The physical properties of immunoreactive cells often change dramatically during activation; therefore,

their baseline characterization has to be carried out using passive cells. Passive, resting leukocytes are generally identified by their quiescence and spherical shape. Unless stated otherwise, we took special care to keep the J774 macrophages in a passive state throughout the mechanical manipulations imposed by our experiments.

As a first important result, we found that J774 cells that had been removed from adherent cell-culture flasks by scraping were not truly passive but instead in a pre-active or “primed” state, manifested by an easy excitability and a large spread in the observed mechanical properties. J774 cells grown in an adherent layer, therefore, are much less suited for baseline mechanical measurements than cells cultured in suspension. All results reported below were obtained with J774 cells that had been grown in suspension in 50 mL bioreactor tubes placed on a bottle roller.

As with other immune cells, activation of J774 macrophages may be triggered by mechanical stimulation or by contact with surfaces recognized as “foreign”. We implemented several additional measures to diminish cell activation. First, the tendency of J774 cells to activate was considerably reduced by carrying out the experiments in a calcium-free buffer. Further, the addition of 10% FBS to the experiment buffer decreased cell activation caused otherwise by cell contact with the bare glass surfaces of the bottom coverslip and the pipette. However, it was only after we began to use PEG-silanized bottom coverslips and SurfaSil-treated micropipettes that cell activation became a rare event within the timeframe of our mechanical experiments. Even so, prolonged manipulation still caused some cells to start activating, evincing that our treatment did not irreversibly affect the cells’ potential for autonomous deformation. Any results obtained from cells exhibiting signs of activation were excluded from the analyses presented in the next two sections.

Behavior of the cortical tension of passive J774 macrophages

To establish the tension-versus-area behavior of passive J774 macrophages, individual cells were partially aspirated at known suction pressures Δp in glass micropipettes with inner diameters of ~5 μm (Figs. 1 and 2 A). Each cell initially was allowed to reach a stationary projection length L_p at a low holding pressure. Subsequently, the pressure was

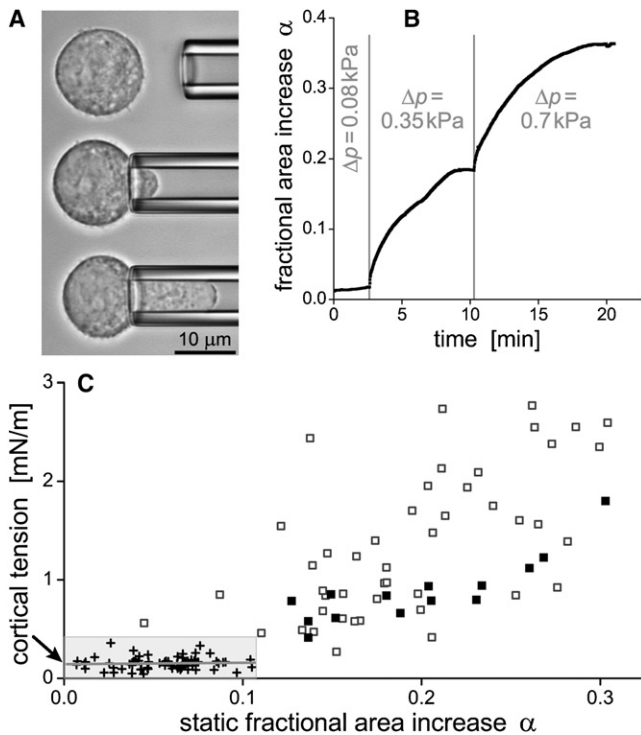


FIGURE 2 Behavior of the cortical tension of passive J774 cells during an externally imposed area increase. (A) The cells were deformed by partial aspiration in a micropipette. (B) Typical time dependence of the fractional area increase in response to steps in suction pressure Δp . (C) The cortical tension of J774 cells rose with increasing static values of α . Small-deformation data (+, shaded box) were used to determine the cortical resting tension (at $\alpha = 0$, arrow). At larger deformations (\square , \blacksquare), the amount of scatter was smaller when only those experiments were considered in which the nucleus visibly remained outside of the pipette (\blacksquare). Results from a total of 65 cells were included in this graph.

increased in one to two steps and held constant after each step for ~ 5 –15 min. The resulting fractional area increase (Fig. 2 B) was given by the two-dimensional strain

$$\alpha = (A - A_0)/A_0, \quad (1)$$

where A is the visible, macroscopic cell surface area (disregarding its irregular microstructure), and A_0 is the area of the undeformed, passive spherical cell. The surface area was calculated from the projection length L_p (that was tracked automatically in the video images as explained by Heinrich and Rawicz (11)), assuming that the cell volume remained constant throughout the experiment, and that the cell geometry could be well described by spherical and cylindrical parts. Fig. 2 B shows how α gradually reaches a new plateau after each pressure step. This was the predominant behavior in experiments carried out in calcium-free medium (with ~ 1 mM EDTA). In buffer containing calcium, we found that a considerable fraction of aspirated cells began to actively move into or out of the pipette during the long holding times. (Those cells were excluded from the analysis.)

For each stationary value of α , we calculated the isotropic cortical tension $\underline{\sigma}$ of the J774 cells using Laplace's law, expressed as

$$\underline{\sigma} = 1/2 \Delta p R R_p / (R - R_p) \quad (2)$$

for aspirated fluid-membrane capsules (for notation see Fig. 1 A). The tension is plotted as a function of stationary α -values in Fig. 2 C, showing a clear upward trend at increasing α . We extracted the cortical resting tension from these data by fitting a straight line to the low-pressure values ($\alpha \leq \sim 0.12$, $\underline{\sigma} \leq \sim 0.4$ mN/m). The intercept (marked by an arrow in Fig. 2 C) gave a resting tension of ~ 0.14 (± 0.2) mN/m. The slope of the initial tension increase was ~ 0.15 mN/m (but with an error about twice as large).

When comparing the J774 cortical resting tension with values published for neutrophils, it is important to recall that previous analyses often assumed a constant cortical tension and thus gave the average of individual measurements, which generally is higher than the extrapolated $\alpha = 0$ value we report. Using the same method of analysis as described here, the resting tension of human neutrophils was found to be as low as 0.011–0.015 mN/m (7) and 0.024 mN/m (12). Therefore, the resistance of passive J774 cells to expansion of their surface areas is about one order of magnitude higher than that of human neutrophils.

The apparent tension values at larger deformations (Fig. 2 C) illustrate the effect of the nucleus of J774 cells. Higher pressures were usually required to further aspirate a cell whose nucleus had partially entered the pipette. This effect is due to the stiffness of the nucleus and does not necessarily reflect a higher tension of the cell cortex. A better estimate of the cortical tension at larger deformations is given by the solid squares, marking cases where the nucleus remained in the spherical cell part outside the pipette.

Cytoplasmic viscosity of passive J774 macrophages

A different type of aspiration experiment (13–15) was carried out to independently estimate the ratio between the cortical tension ($\underline{\sigma}$) and the cytoplasmic viscosity η of J774 macrophages (Fig. 3). For passive cells, this ratio determines the dynamics of cell recovery to a spherical shape after deformation. We subjected individual J774 cells to a well-defined deformation by fully aspirating them into wider pipettes (8.3–10.5 μ m diameter; Fig. 3, A and B). Each cell was held inside the pipette for 10 s, then gently released into the experiment chamber. Cell recovery to a (nearly) spherical shape usually took 2–5 min and was quantified by measuring the length and width of the recovering cell as a function of time (Fig. 3 C).

The classical cortical shell-liquid core model of leukocyte viscoelasticity (16) has been superseded by more refined models in recent years (17); however, in particular the implementation by Tran-Son-Tay et al. (15) remains a useful tool

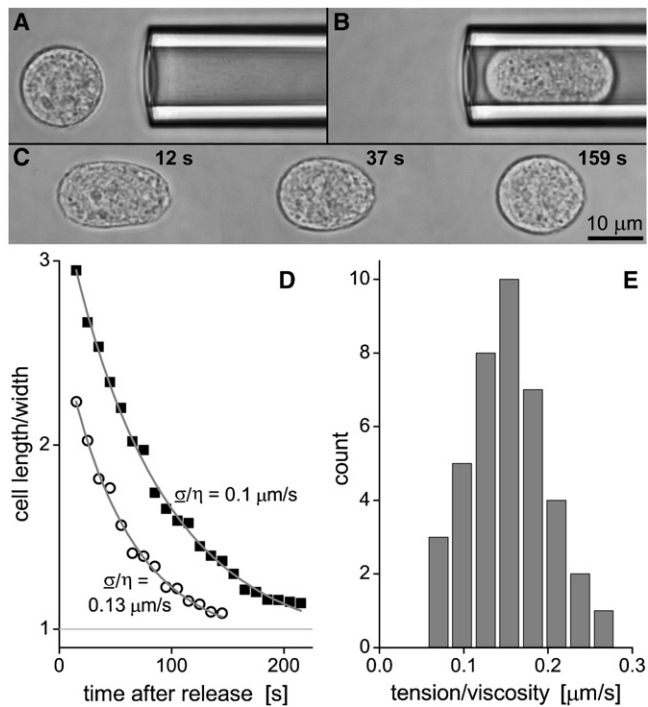


FIGURE 3 Measurement of the ratio between the cortical tension $\underline{\sigma}$ and the cytoplasmic viscosity η of passive J774 cells. (A–C) Each cell was fully aspirated into a large pipette, then held for 10 s, and finally released to examine the time course of cell recovery. (D) The measured ratio of cell length/width during recovery was plotted for two examples as a function of time and fit with a model adapted from Tran-Son-Tay et al. (15), where one of the fitting parameters was $\underline{\sigma}/\eta$. (E) The histogram of all measurements (using a total of 40 cells) exposed a most frequently observed value of $\underline{\sigma}/\eta = 0.15 \mu\text{m/s}$.

in the practical interpretation of cell-recovery measurements. That analysis provided an approximate analytical solution to the equations of creeping flow of a Newtonian droplet with a moving, prestressed boundary. Slightly modifying the original analysis, we adopted this approximation to model the time dependence of the ratio of length/width of the recovering J774 macrophages as shown in Fig. 3 D (taking note, however, that the model assumes a constant cortical tension and neglects viscous contributions of the cell cortex and the nucleus).

This approach yielded reasonable fits to our data, giving as one fitting parameter a rough estimate of the ratio $\underline{\sigma}/\eta$. We collected the measured values of this ratio into the histogram shown in Fig. 3 E, showing a most frequent value of $\underline{\sigma}/\eta = 0.15 \mu\text{m/s}$. Identifying $\underline{\sigma}$ with the independently measured cortical resting tension (see Fig. 2), we obtain a cytoplasmic viscosity of passive J774 cells of approximately $\eta = 0.93 \text{ kPa}\cdot\text{s}$ at room temperature, $\sim 5\text{--}10$ times higher than that of human neutrophils. Interestingly though, the ratio $\underline{\sigma}/\eta$ of J774 macrophages is close to the value obtained for human leukocytes (18). We hypothesize that this ratio may be conserved across various types of immune cells, indicating that a tight balance between cortical tension and interior cell

viscosity is an important prerequisite for the motile aptitude of these cells.

Stiffness of passive cells contrasts with vast membrane reserves recruited during active deformation

The above measurements established that passive J774 cells resist expansion of their surface area ~ 10 times more strongly than neutrophils. One might expect, therefore, that the capacity of these cells to increase their total apparent surface area during active deformation is smaller than that of neutrophils. In contrast, we observed a surprising ability of J774 macrophages to call on immense reserves of surface area during phagocytosis.

To estimate the maximum total surface area increase of J774 cells, we used their aptitude to engulf Fc γ -opsonized targets. We used our pipette-manipulation setup to bring large, antibody-coated beads (diameter $\sim 20 \mu\text{m}$) into contact with individual macrophages, which usually resulted in immediate adhesion and subsequent phagocytosis of the bead. Although the initial cell diameter of the resting spherical cells ($\sim 15\text{--}18 \mu\text{m}$) was smaller than the bead diameter, macrophages had no problem engulfing two $20\text{-}\mu\text{m}$ beads (Fig. 4 A), and proceeded to tackle a third bead when offered (Fig. 4 B). At that point, the pseudopods surrounding the third bead became too thin to be reliably observed in an optical microscope; however, partial bead engulfment was clearly visible.

Assuming that the outer surfaces of the engulfed beads were initially covered by a double layer of cell membrane, we can estimate the final surface area from simple geometry. We found that the surface area of J774 cells such as shown in Fig. 4 easily increased to more than five times of the initial area of the resting, spherical cell. This area increase is

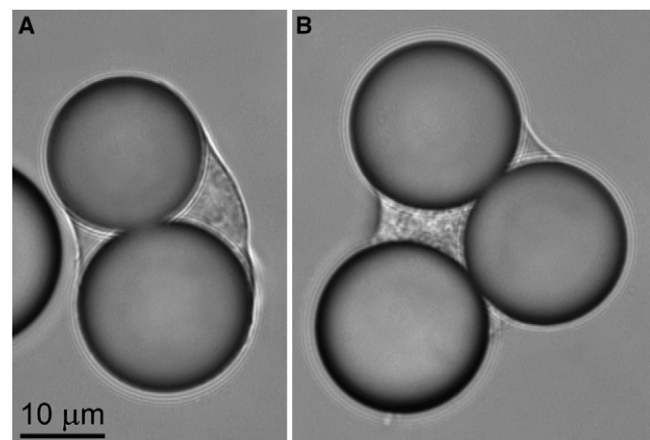


FIGURE 4 Video micrographs of phagocytosis of Fc γ -opsonized $20 \mu\text{m}$ (nominal diameter) beads by J774 macrophages. (A) An initially spherical (resting diameter $15.8 \mu\text{m}$) J774 cell has fully engulfed two beads. (B) A J774 macrophage (initial diameter $16.8 \mu\text{m}$) has fully engulfed two beads, and a third one partially.

considerably larger than the maximum ~ 3 -fold increase observed during phagocytosis by neutrophils.

To examine how macrophages recruit such enormous additional, apparent surface area reserves, we proceeded to take scanning electron microscope (SEM) images of J774 cells that had been incubated with even larger antibody-coated polystyrene beads (nominal diameter $\sim 30 \mu\text{m}$). Snapshots of adherent, resting J774 cells (Fig. 5) confirm that the surface of passive macrophages has a highly irregular structure, consisting of a remarkable multitude of membrane wrinkles (19). At the onset of phagocytosis, the activating cells initially seem to develop more pronounced surface ruffles, presumably through the coalescence of finer wrinkles into larger membrane folds. However, when the J774 cells are confronted with $\text{Fc}\gamma$ -opsonized targets whose surface area is ~ 3 times as large as their own, the ruffles eventually will be ironed out, i.e., their membrane gradually will be incorporated into the growing, increasingly smooth, apparent cell-surface area (Fig. 6). Images like the bottom micrograph of Fig. 6 confirm that individual J774 macrophages are capable of fully engulfing beads as large as $\sim 30 \mu\text{m}$. Because the original cell diameter is unknown in these SEM images, we cannot determine the surface-area increase of individual phagocytes; however, it is instructive to note that a macrophage with a resting diameter of $18 \mu\text{m}$ has to increase its apparent surface area ~ 5.5 times to fully surround a $30 \mu\text{m}$ (diameter) bead with a double layer of membrane.

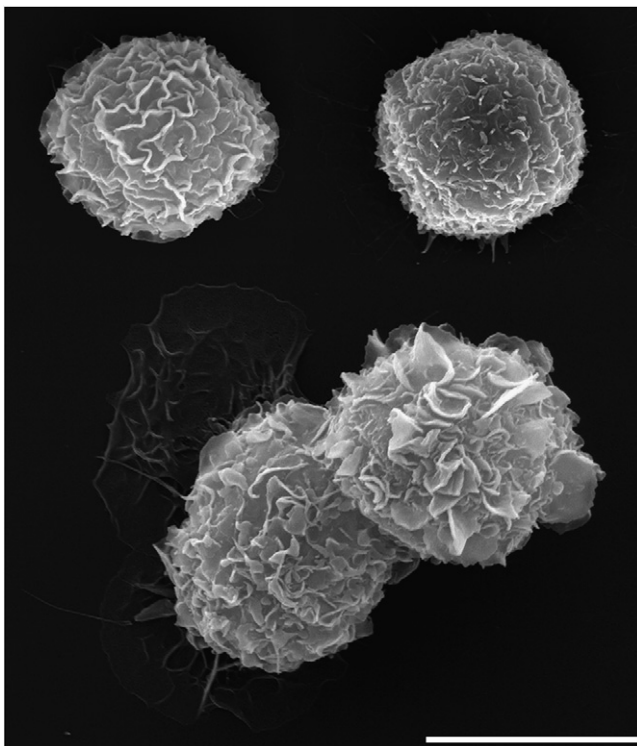


FIGURE 5 Collage of SEM micrographs of resting J774 macrophages. Scale bar = $10 \mu\text{m}$ (note that the cell size is not representative due to some shrinkage during fixation).

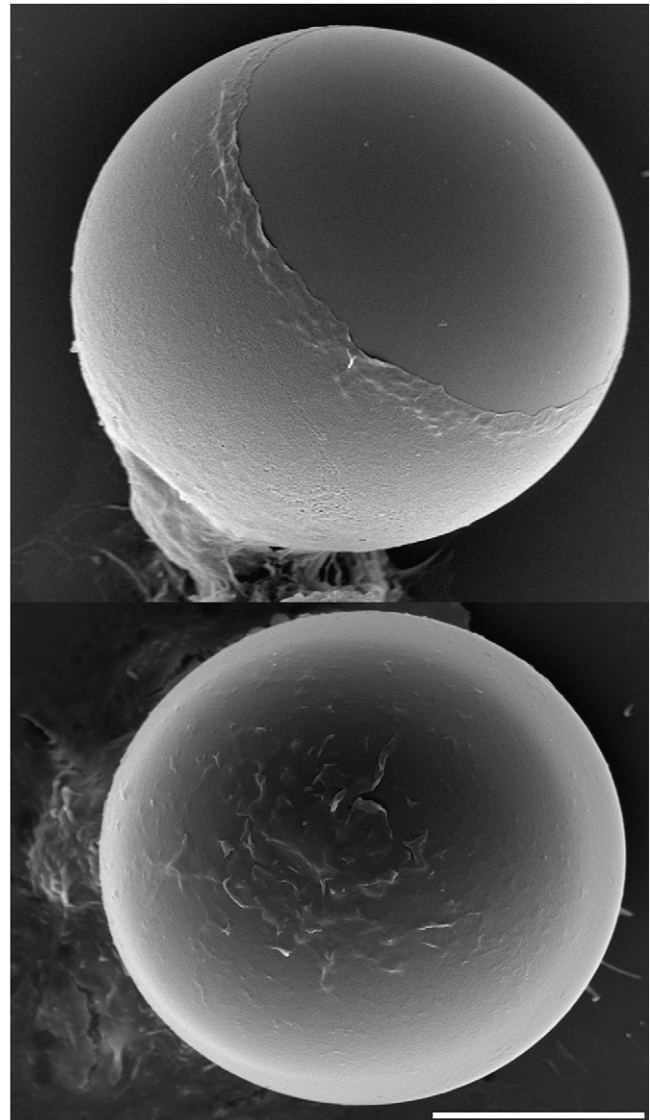


FIGURE 6 Composite of two SEM micrographs of J774 macrophages engulfing $\text{Fc}\gamma$ -opsonized $30 \mu\text{m}$ (nominal diameter) beads. Whereas the macrophage at the top is still in the process of engulfment, the bottom cell has fully enclosed the target bead. Scale bar = $10 \mu\text{m}$.

CONCLUSIONS

Macrophage cell lines, in addition to their prominence in immunological studies, are ideal model systems for biophysical analyses of cellular processes like phagocytosis and chemotaxis, potentially offering a wealth of new insight into the mechanistic foundations of eukaryotic cell motility. In this study, we have conducted micromechanical experiments on murine J774 macrophages to establish the baseline mechanical behavior of these cells, i.e., their cortical resting tension, static tension-versus-surface-area relationship, effective cytoplasmic viscosity, and available surface-area reserve. These properties represent a useful common denominator for comparative studies of different forms of autonomous deformation by various motile cell types (7–10,20,21). For

example, comparing our results with previous studies on human neutrophils, we found that both the resting cortical tension of J774 cells as well as their cytoplasmic viscosity are about one order of magnitude higher than the respective neutrophil values. This difference underlines the need for careful examination of variations in the behavior of different types of motile immune cells. Such an analysis shall eventually enable us to distinguish whether the variations are caused by qualitatively distinct mechanisms, or by the modulation of a universal mechanistic program of autonomous cell deformation.

To relate the biophysical insights gained from our measurements to their physiological context, it is important to recall the distinction between the macroscopic, apparent surface area of leukocytes, and the actual cell membrane that is highly irregular on the microscale. The former is the visible (in an optical microscope; Figs. 1–4) surface area of the cell envelope, whereas the latter (Fig. 5) can be considered to provide an extensive membrane reservoir that likely consists of several compartments. Beside the microscopic wrinkles of the cell surface, additional candidates for such compartments include internal vesicles and the endoplasmic reticulum. The wrinkles themselves may also be of distinct types and belong to more than one compartment (as postulated for neutrophils in Herant et al. (7)).

Starting from this picture, one may speculate about the microscopic origins of the macroscopic behavior of the J774 cortex documented in Fig. 2 C. First, the nonvanishing cortical resting tension attests to the persistent maintenance of the membrane reservoir by the idling machinery of passive cells. We envision, for instance, that the surface wrinkles are stabilized by cross-linking cytoskeletal filaments that undergo a continual dynamic renewal. Likewise, there is turnover of membrane between the cell surface and endovesicles (6,22–24). Next, the two-dimensional, static stress-strain relationship of Fig. 2 C seems to be biphasic, qualitatively similar to what we found for neutrophils. The observed slack at low tensions changes to an elastic-like dilation of the apparent surface area at higher tensions, with the transition at ~10–15% area expansion. This suggests that J774 cells recruit their surface area from at least two different membrane compartments at these tensions, possibly from two classes of membrane wrinkles, i.e., weakly and strongly cross-linked ones (7). The slack at low tensions enables the cells to accommodate small deformations with relative ease. However, shape changes of deformed passive cells beyond a ~15% area increase become energetically more costly because they are opposed by an elevated cortical tension. This tendency to minimize the cell-surface area is responsible for maintaining the spherical shape of passive cells.

Features that are conserved in the mechanical behavior of macrophages and neutrophils are likely to be involved—perhaps critically—in physiological processes that are common to these immune cells. We thus reason that the observed, qualitatively similar properties, i.e., the nonvanishing resting

tension and the biphasic stress-strain relation of the cell cortex, are important for the capability of autonomous deformation of these cells. An even more intriguing, quantitative similarity between J774 macrophages and human leukocytes (18) is shown in their ratio of tension/viscosity, $\underline{\sigma}/\eta$. We hypothesize that the closeness of the respective values is unlikely to be a coincidence, but instead may indicate a physically constrained, tightly conserved balance between the cortical tension and cytoplasmic viscosity of different types of immune cells. Such a tight balance is not surprising given the motile aptitude of these cells. It makes sense that the interior viscosity cannot be too low at a given tension; otherwise, the cell body would not be able to provide bracing support for developing protrusions. Conversely, if the interior viscosity was too high, it would preclude the tension-driven propensity of the cell to round up (within a reasonable amount of time) when returning to a passive state.

On the other hand, a particularly stark and somewhat unexpected contrast between J774 cells and human neutrophils becomes evident if one views their different capacity for active surface-area recruitment in the context of their 10-fold difference in passive stiffness. We find that macrophages possess immense additional membrane reserves, allowing them to expand their apparent surface area more than five times during the engulfment of large, antibody-coated targets (Figs. 4 and 6). The inspection of SEM micrographs (Figs. 5 and 6) shows that the highly irregular plasma membrane of resting J774 cells stores a vast amount of area, which eventually is recruited into the increasingly smooth cell surface during phagocytosis. Our results currently do not allow us to quantify the contributions of other possible membrane-storage compartments, such as the endoplasmic reticulum, whose proposed role in phagocytosis (25) has been disputed recently (6). However, in view of the turnover of membrane between the plasmalemma and internal vesicles (6,22–24), we expect the equilibrium between these two compartments to shift toward the plasma membrane whenever the cell surface needs to expand significantly. Overall, it seems plausible to assume that the J774 macrophages will eventually mobilize every reserve they can to achieve the remarkable greater than fivefold increase in surface area. Interestingly, if one extrapolates the data of Fig. 2 C to a fivefold area increase, the predicted tension will be larger than the typical lysis tension of lipid membranes (26). Thus our results show that active cells use special mechanisms to regulate their surface area and tension.

Our results necessarily involve a number of assumptions. The interpretation of our cell-recovery experiments (Fig. 3) is based on the cortical shell-liquid core model (16) of leukocyte viscoelasticity. Although this classical model captures some of the main mechanical properties of leukocytes, it was not intended to describe others (17,27). One of its assumptions is that the cell cortex exhibits a persistent, constant tension, which is contradicted by the results of Fig. 2 and our previous experiments on human (7) and mouse

(28) neutrophils, as well as by other studies (12). Yet at small deformations, the surfaces of both neutrophils and J774 macrophages exhibit a certain amount of slack, i.e., their initial area expansion occurs at a very slow rise of the cortical tension. Therefore, the assumption of constant tension should be a reasonable approximation as long as the imposed cell deformation remains small. We also reiterate that our experiments were carried out at room temperature, in keeping with almost all existing biomechanical studies on leukocytes. Two previous micropipetting studies examined the temperature dependence of the cytoplasmic viscosity (29) and the cortical tension (30) of neutrophils, respectively. Given the qualitatively similar behavior of passive neutrophils and J774 cells, we speculate that the mechanical properties of these two cell types exhibit similar temperature dependences as well.

We are grateful to C. Ounkomol for preparing the sketch of the aspiration setup in Fig. 1 B.

This work was supported by National Institutes of Health grant R01 A1072391.

REFERENCES

- Ralph, P., and I. Nakoinz. 1975. Phagocytosis and cytolysis by a macrophage tumour and its cloned cell line. *Nature*. 257:393–394.
- Ralph, P., and I. Nakoinz. 1977. Antibody-dependent killing of erythrocyte and tumor targets by macrophage-related cell lines: enhancement by PPD and LPS. *J. Immunol.* 119:950–954.
- Unkeless, J. C., G. Kaplan, H. Plutner, and Z. A. Cohn. 1979. Fc-receptor variants of a mouse macrophage cell line. *Proc. Natl. Acad. Sci. USA*. 76:1400–1404.
- Kant, A. M., P. De, X. Peng, T. Yi, D. J. Rawlings, et al. 2002. SHP-1 regulates Fc γ receptor-mediated phagocytosis and the activation of RAC. *Blood*. 100:1852–1859.
- Aderem, A. 2002. How to eat something bigger than your head. *Cell*. 110:5–8.
- Touret, N., P. Paroutis, M. Terebiznik, R. E. Harrison, S. Trombetta, et al. 2005. Quantitative and dynamic assessment of the contribution of the ER to phagosome formation. *Cell*. 123:157–170.
- Herant, M., V. Heinrich, and M. Dembo. 2005. Mechanics of neutrophil phagocytosis: behavior of the cortical tension. *J. Cell Sci.* 118:1789–1797.
- Herant, M., V. Heinrich, and M. Dembo. 2006. Mechanics of neutrophil phagocytosis: experiments and quantitative models. *J. Cell Sci.* 119:1903–1913.
- Hallett, M. B., and S. Dewitt. 2007. Ironing out the wrinkles of neutrophil phagocytosis. *Trends Cell Biol.* 17:209–214.
- Swanson, J. A. 2008. Shaping cups into phagosomes and macropinosomes. *Nat. Rev. Mol. Cell Biol.* 9:639–649.
- Heinrich, V., and W. Rawicz. 2005. Automated, high-resolution micropipet aspiration reveals new insight into the physical properties of fluid membranes. *Langmuir*. 21:1962–1971.
- Needham, D., and R. M. Hochmuth. 1992. A sensitive measure of surface stress in the resting neutrophil. *Biophys. J.* 61:1664–1670.
- Dong, C., R. Skalak, K. L. Sung, G. W. Schmid-Schonbein, and S. Chien. 1988. Passive deformation analysis of human leukocytes. *J. Biomech. Eng.* 110:27–36.
- Sung, K. L., C. Dong, G. W. Schmid-Schonbein, S. Chien, and R. Skalak. 1988. Leukocyte relaxation properties. *Biophys. J.* 54:331–336.
- Tran-Son-Tay, R., D. Needham, A. Yeung, and R. M. Hochmuth. 1991. Time-dependent recovery of passive neutrophils after large deformation. *Biophys. J.* 60:856–866.
- Yeung, A., and E. Evans. 1989. Cortical shell-liquid core model for passive flow of liquid-like spherical cells into micropipets. *Biophys. J.* 56:139–149.
- Herant, M., W. A. Marganski, and M. Dembo. 2003. The mechanics of neutrophils: synthetic modeling of three experiments. *Biophys. J.* 84:3389–3413.
- Lim, C. T., E. H. Zhou, and S. T. Quek. 2006. Mechanical models for living cells—a review. *J. Biomech.* 39:195–216.
- Petty, H. R., D. G. Hafeman, and H. M. McConnell. 1981. Disappearance of macrophage surface folds after antibody-dependent phagocytosis. *J. Cell Biol.* 89:223–229.
- Kay, R. R., P. Langridge, D. Traynor, and O. Hoeller. 2008. Changing directions in the study of chemotaxis. *Nat. Rev. Mol. Cell Biol.* 9:455–463.
- Hallett, M. B., C. J. von Ruhland, and S. Dewitt. 2008. Chemotaxis and the cell surface-area problem. *Nat. Rev. Mol. Cell Biol.* 9:662.
- Cox, D., D. J. Lee, B. M. Dale, J. Calafat, and S. Greenberg. 2000. A Rab11-containing rapidly recycling compartment in macrophages that promotes phagocytosis. *Proc. Natl. Acad. Sci. USA*. 97:680–685.
- Wustner, D. 2007. Plasma membrane sterol distribution resembles the surface topography of living cells. *Mol. Biol. Cell*. 18:211–228.
- Wustner, D., M. Mondal, I. Tabas, and F. R. Maxfield. 2005. Direct observation of rapid internalization and intracellular transport of sterol by macrophage foam cells. *Traffic*. 6:396–412.
- Gagnon, E., S. Duclos, C. Rondeau, E. Chevet, P. H. Cameron, et al. 2002. Endoplasmic reticulum-mediated phagocytosis is a mechanism of entry into macrophages. *Cell*. 110:119–131.
- Evans, E., V. Heinrich, F. Ludwig, and W. Rawicz. 2003. Dynamic tension spectroscopy and strength of biomembranes. *Biophys. J.* 85:2342–2350.
- Drury, J. L., and M. Dembo. 2001. Aspiration of human neutrophils: effects of shear thinning and cortical dissipation. *Biophys. J.* 81:3166–3177.
- Kim, S. V., W. Z. Mehal, X. Dong, V. Heinrich, M. Pypaert, I, et al. 2006. Modulation of cell adhesion and motility in the immune system by Myo1f. *Science*. 314:136–139.
- Evans, E., and A. Yeung. 1989. Apparent viscosity and cortical tension of blood granulocytes determined by micropipet aspiration. *Biophys. J.* 56:151–160.
- Liu, B., C. J. Goergen, and J. Y. Shao. 2007. Effect of temperature on tether extraction, surface protrusion, and cortical tension of human neutrophils. *Biophys. J.* 93:2923–2933.